

## Article

# Response of the Stability of Soil Aggregates and Erodibility to Land Use Patterns in Wetland Ecosystems of Karst Plateau

Longpei Cen <sup>1</sup>, Xudong Peng <sup>1,2,\*</sup>  and Quanhou Dai <sup>1,2,3</sup>

<sup>1</sup> College of Forestry, Guizhou University, Guiyang 550025, China; gs.lpcen21@gzu.edu.cn (L.C.); qhdai@gzu.edu.cn (Q.D.)

<sup>2</sup> Institute of Soil Erosion and Ecological Restoration, Guizhou University, Guiyang 550025, China

<sup>3</sup> Guizhou Karst Environmental Ecosystems Observation and Research Station, Ministry of Education, Guiyang 550025, China

\* Correspondence: xdpeng@gzu.edu.cn; Tel.: +86-15208515946

**Abstract:** The world's natural wetlands, which have important ecological functions, are being lost at an alarming rate. The erosion and deposition of soil on wetlands is a major cause of wetland conversion to agriculture. An urgent problem to be solved is how to slow down the erosion and deposition of wetlands resulting from land use. Land use patterns affect soil properties, thereby affecting soil aggregate stability and erodibility. Evaluating the effects of land use patterns on soil aggregate stability and erodibility in small watersheds of wetland ecosystems of karst plateau is of great importance. Thus, we compared the soil properties, aggregate stability indicators and soil erodibility of shrubland, grassland, artificial forest land and sloping farmland for evaluating the impact of various land use patterns on soil aggregate stability and erodibility in typical karst plateau wetland ecosystems. Our results showed that the mass fraction of soil aggregates > 0.25 mm was the main component in the four land uses, with greater variation in aggregates > 5 mm; overall, MWD, GMD and WSA<sub>0.25</sub> were higher in grassland and shrubland than in sloping farmland and artificial forest land, while K values, PAD and SCAI showed the opposite trend. Correlation analysis showed that effective soil nutrients had a positive effect on soil aggregate stability. In conclusion, the stability of soil aggregates and resistance to soil erosion were strongest under the influence of shrubland. Our study showed that shrubland can better improve soil aggregate stability and erosion resistance, which may provide a guide for protecting and restoring karst plateau wetland ecosystems.

**Keywords:** soil aggregate stability; soil erodibility; land use patterns; wetland ecosystems; karst plateau



**Citation:** Cen, L.; Peng, X.; Dai, Q. Response of the Stability of Soil Aggregates and Erodibility to Land Use Patterns in Wetland Ecosystems of Karst Plateau. *Forests* **2024**, *15*, 599. <https://doi.org/10.3390/f15040599>

Academic Editors: Choonsig Kim and Lei Deng

Received: 28 January 2024

Revised: 22 March 2024

Accepted: 25 March 2024

Published: 26 March 2024



**Copyright:** © 2024 by the authors. Licensee MDPI, Basel, Switzerland. This article is an open access article distributed under the terms and conditions of the Creative Commons Attribution (CC BY) license (<https://creativecommons.org/licenses/by/4.0/>).

## 1. Introduction

Wetlands are one of the most important ecological systems and habitats for many organisms on Earth. Wetlands around the world are being lost at an alarming rate due to global climatic change, soil erosion and human activities (such as agriculture and lake reclamation). Over the last three centuries, about 3.4 million square kilometres (2% of the Earth's land area) of wetlands have been lost, mainly to rice and marshland [1]. Soil loss is the most widespread land degradation process worldwide [2,3] and is one of the key drivers of wetland agriculturalization. Caohai is not only one of the world's top ten plateau wetlands, but also one of the few natural freshwater plateau lakes in a similar latitude on Earth. It is an important natural resource with unique characteristics and global importance [4,5]. However, human activities and changes in land use have exacerbated soil erosion, seriously threatening Caohai's ecological stability in recent years. The stability and erodibility of soil aggregates are important for the prediction of soil water loss and soil erosion [6,7]. Therefore, studying the stability of soil aggregates is crucial to protect productive capacity and minimise soil erosion and environment pollution caused by soil deterioration [8–10].

Land use pattern is an important determinant of soil quality, as land use changes soil structure, nutrient and microbial properties over time [11,12]. As one of the physical properties of soil, soil aggregate stability is an essential indicator for evaluating soil quality and a measure of soil degradation under land use change [6]. Research has indicated that land use patterns affect the soil aggregate stability [7,13]. For example, grassland and forest have higher soil aggregate stability than agricultural land and bare land [7,14,15].

Studies conducted in recent decades have also mainly explored the impacts on soil aggregates of restoration of vegetation, soil type and tillage type, and they have produced results [9,13,16–18]. For example, natural shrub aggregates exhibited the best stability, according to Dou et al. (2020) [13] investigated the influence of various vegetation restoration techniques on the stability of soil aggregates in the Loess Plain. Furthermore, soil aggregate stability and related nutrient dynamics have also been studied [19–21]. However, previous studies have failed to consider widely applicable indicators for the assessment of soil aggregate stability [18,22], and the stability of soil aggregation under various land use patterns in small watersheds of karst wetland ecosystems is still unknown.

Furthermore, soil erodibility describes the difficulty of eroding the soil and indicates the soil's susceptibility to erosion and migration caused by external erosion [23]. Studies have shown that the main drivers of soil erodibility variation with land use pattern are soil and plant characteristics [24]. Wang et al. (2019) [24] and Chen et al. (2023) [25] evaluated soil erosion variation with land use pattern in typical small watersheds in the Loess Plateau and Northeast China, respectively. The results showed that shrubland and the horizontal forest belt had the lowest soil erodibility. The soil erodibility of fenced grassland was shown to be low by Zhou et al. (2022) [18]. USLE, EPIC, RUSLE2 and other models are often used for karst soil erodibility studies to evaluate erodibility of large and medium basins [10,26]. Thus, differences in land use patterns in different regions and resulting vegetation and climate changes often result in non-universality of erodibility of soil aggregates [25]. Due to the effect of region, land use pattern, slope and other environmental variables, most researchers have studied soil aggregate stability and erodibility in different regions and land use patterns, with slightly different results [17]. Moreover, reports on soil aggregates in karst areas have not combined various land use patterns to comprehensively evaluate soil aggregate stability and erodibility, especially in karst plateau wetland ecosystems.

Global wetland area worldwide has decreased dramatically in recent years due to climatic change and the rapid expansion of agriculture, which has negatively impacted the function of wetland ecosystems [27]. Caohai Lake is a typical Chinese subtropical karst plateau wetland ecosystem, and its ecological milieu is highly representative in terms of its vulnerability, typicality, significance and biodiversity [28] and has also faced serious threats to its ecological environment. On the one hand, the surface around the Caohai Lake basin is exposed and precipitation in Caohai more concentrated, and high surface runoff and strong soil erosion cause the accumulation of large amounts of sediment to be carried into the lake [29]. On the other hand, change in land use patterns/ human activities have created environmental problems like soil erosion in recent decades, seriously threatening the sustainability of wetland ecosystems themselves and their ecological services [30,31]. Soil erosion is a primary contributor to land degradation, and land use patterns are an important factor influencing the intensity of soil erosion and its spatial distribution [3,32]. Therefore, studying the stability and erodibility of soil aggregates is crucial for comprehending the impact of land use patterns on soil erosion in the region to help maintain the stability of the ecosystem and improve its service function. However, the understanding of the effects of various land use patterns on soil aggregate stability and soil erodibility remains limited. How do land use patterns in the surrounding sub-basins of the Caohai ecosystem change soil aggregate stability and soil erodibility? What land use patterns are most effective in improving soil aggregate structure? Therefore, it is necessary to evaluate the spatial changes in soil aggregate stability and erodibility under different land uses to help determine appropriate land use patterns to reduce soil erosion and land degradation, thereby maintaining the stability of the ecosystem and enhancing its service functions.

We selected four land use types for their effect on soil aggregate stability and erodibility in small watersheds of a typical karst plateau wetland ecosystem. The study aimed to do as follows: (1) analyse the effects of different land use patterns on the distribution of soil aggregate components and the water stability of aggregates; (2) explore the response of soil erodibility to different land use patterns and evaluate which land use pattern is most effective in improving soil erosion resistance. These results may provide a basis for further evaluation of the protection and restoration of karst plateau wetland ecosystems.

## 2. Materials and Methods

### 2.1. Study Area

The research region is located in the Shahe small watershed (E 104°17′–104°18′, N 26°50′–26°51′) near the Caohai Wetland Conservation Area in Caohai Town, Weining Yi, Miao and Hui Autonomous County, Guizhou Province, China. The watershed has a land area of about 1.12 km<sup>2</sup>, a length from north to south of 1243 m, a width from east to west of 1109 m, a maximum elevation of 2311 m, a minimum elevation of 2182 m and a relative altitude of 125 m. The average annual temperature is 10.6 °C, the average annual rainfall is 950 mm and the average annual sunshine is 1805.4 h. The study area belongs to a karst and denuded hilly terrain, with a steamed-bun-shaped hilltop extending from east to west, and sandstone and dolomite as bedrock. Yellow soil (classified in the FAO Taxonomy as Haplic Acrisol) is the soil type. The main land use patterns in the study area are artificial forest land (AFL), shrubland (SL), sloping farmland (SF), and grassland (GL). Sloping farmland and grassland are the two main areas of economic value in the region. Artificial forest land has Yunnan Pine (*Pinus Yunnanensis*) and Huashan Pine (*Pinus armandii Franch*) as the main vegetation. In shrubland, firethorn (*Pyracantha fortuneana*) and huckleberry (*E. pungens*), are dominant, with a plant height of about 2.2 m and a vegetation cover of 46%. AFL and SL slopes are mainly 5–15°, and some AFL and SL slopes reach 15–25°. Sloping farmland has an average slope of 5–10°, 77% of which is prone to soil erosion, with maize (*Zea mays*) and potatoes (*Solanum tuberosum*) as the main crops. Grassland, with an average slope of 5–10°, with ryegrass (*Lolium perenne* L.) and alfalfa (*Medicago sativa*) as the main crops, is the main pasture for sheep farms. AFL and SL have a limited community structure, low vegetation cover, poor vegetation growth, thin soil layers and serious soil sandification.

### 2.2. Soil Sampling and Treatments

#### 2.2.1. Experimental Design and Field Sampling

Sampling plots were set up in the Shahe small watershed of the Caohai wetland on the Guizhou karst plateau (Figure 1 and Table S1). We adopted the grid method for sampling site distribution, that is, two adjacent sampling sites were separated by 100 m. Sampling was carried out using the 'S' method, taking five 0–20 cm soil samples within a 10 m radius of the grid site and mixing these five samples into one mixed sample representing the plot. The GPS was used to record the specific geographical data of the sampling plots and to determine the specific location of the sampling sites. A total of 70 sampling plots (15 GL, 20 SL, 22 SF and 13 AFL) were collected in plastic baggies and taken to the laboratory. The soil samples for the determination of soil physicochemical properties were ground and sieved through 2 mm and 0.25 mm sieves to remove roots and stones.

The undisturbed soil was brought back to the laboratory in an aluminium box, cleaned of roots and stones, and dried. We then weighed 500 g of the soil samples and obtained 5 mm soil aggregates by dry sieving. According to the proportion of each aggregate size, 50 g mixed soil samples containing different aggregate components were matched, and water stable aggregates of different sizes were obtained by the wet sieving method [18,33].

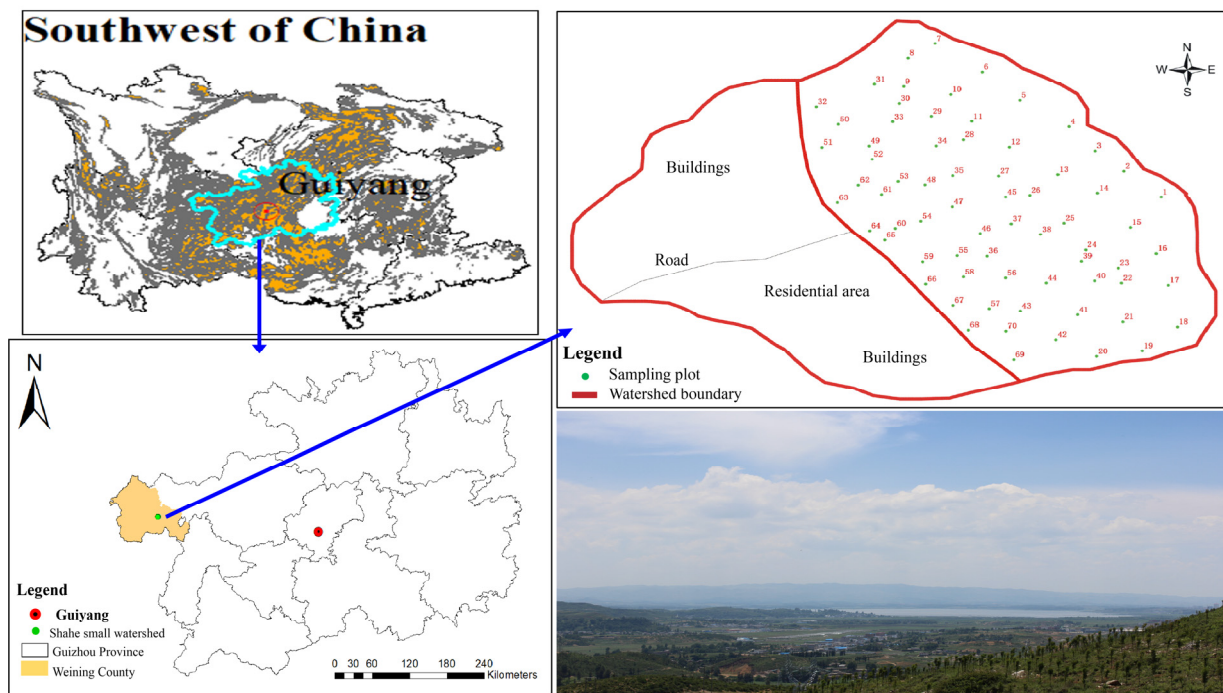


**Figure 1.** The location of the study area. Note: The numbers in the figure represent the sampling point numbers.

Natural soil water content (SWC) was determined by the drying method. Soil bulk density (BD) values were determined by cutting ring water immersion. Soil pH was measured by extraction of liquid from a soil–water mixture (ratio of 1:5) [34]. Soil organic carbon (SOC) content was determined by oxidation with potassium dichromate under external heating. Total nitrogen (TN) was measured by the Kjeldahl method [35], and the available nitrogen (AN) was determined by the Conway method. The total phosphorus (TP) was measured by Mo-Sb colourimetric method, and the available phosphorus (AP) was extracted with  $0.5 \text{ mol}\cdot\text{L}^{-1} \text{ NaHCO}_3$  (pH = 8.5) and then determined by colourimetric analysis.

### 2.2.2. Calculation of Soil Index

Mean weight diameter (MWD), geometric mean diameter (GMD), fractal dimension (D values), the specific gravity of large water stable aggregates proportion ( $WSA_{0.25}$ ), percentage of aggregate destruction (PAD) and SOC cementing agent index (SCAI) [36] were calculated using the following equations:

$$\text{MWD} = \frac{\sum_{i=1}^n (\bar{x}_i y_i)}{\sum_{i=1}^n y_i} \quad (1)$$

$$\text{GMD} = \exp\left(\frac{\sum_{i=1}^n y_i \ln \bar{x}_i}{\sum_{i=1}^n y_i}\right) \quad (2)$$

where  $x_i$  is the  $i$ th aggregate particle size mean diameter, and  $y_i$  is the  $i$ th aggregate particle size weight.

$$(3 - D) \log(d_i / d_{\max}) = \log\left(\frac{W_{(\delta < d_i)}}{W_0}\right) \quad (3)$$

where  $W(\delta < d_i)$  is the cumulative mass of soil particle diameters of less than  $d_i$ , and  $W_0$  is the sum of the masses of all soil particles.

$$\text{PAD} = \frac{W - W'}{W} \times 100\% \quad (4)$$

where  $W$  and  $W_0$  are the dry and wet sieved content, respectively, of  $>0.25 \text{ mm}$  aggregates.

$$WSA_{0.25} = \frac{M_{r>0.25}}{M_T} \times 100\% \quad (5)$$

where  $M_r$  is the content of each aggregate (g), and  $M_T$  is the total content of the aggregates.

$$SCAI = \frac{MWD}{SOC} \quad (6)$$

SOC is soil organic carbon content (%), MWD is the mean weight diameter (mm).

The soil erodibility value ( $K_{\text{Shirazi}}$ ), calculated using the Shirazi formula, correlated strongly with the measured K value in different soil erosion areas in China; the estimated level of soil erodibility (K) in a karst plateau [9,18] were calculated as follows:

$$K_{\text{Shirazi}} = 7.954 \times \left( 0.0017 + 0.0494 \times \exp \left[ -0.5 \times \left( \frac{\log GMD + 1.675}{0.6986} \right)^2 \right] \right) \quad (7)$$

$$K = -0.00911 + 0.55066K_{\text{Shirazi}} \quad (8)$$

### 2.3. Statistical Analysis

To test the significance of SOC, TN, TP, AN, SWC, BD, pH under various land use patterns or between various slope positions, a one-way ANOVA with LSD test was used with a  $p$ -value threshold of less than 0.05 [26]; Pearson correlation test was used to obtain the correlation between the soil agglomerate fraction, MWD, GMD and K value and soil properties, and the significant indicators under various land use patterns were selected for principal component analysis (PCA) to calculate the overall soil agglomerate stability score (F value) [18].

## 3. Results

### 3.1. Basic Physical and Chemical Properties of Soil in Different Land Use Patterns

The basic physical and chemical characteristics of the soils of four land use patterns are shown in Table 1. Overall, results indicated no significant variations in SOC, TN and AN among the four different land use patterns. For TP and AP, SF and AFL were significantly higher than GL and SL. Furthermore, there were no significant variations ( $p < 0.05$ ) in SWC, BD and pH for different slope locations for the different land use patterns. Within the AFL, however, there were slight differences in TP, SWC and pH between slope locations. The results indicated that slope, except for SOC and AP, had a relatively minor influence on physical and chemical properties.

### 3.2. Distribution of Soil Water Stable Aggregate Fractions in Soils

The distribution of soil water stable aggregate fractions differentiated by land use is given in Figure 2. Overall, the proportion of soil aggregate mass of the various land use patterns was mostly concentrated in  $>0.25$  mm. In  $>0.25$  mm, the change of  $>5$  mm was greater, and the maximum value of SL appeared (46.66%), while the change of 5–2 mm, 2–1 mm and 0.5–0.25 mm was relatively stable. For 1–0.5 mm and 0.5–0.25 mm, SF and AFL were significantly higher than GL and SL. For  $<0.25$  mm, SF  $>$  AFL  $>$  GL  $>$  SL. Generally, SL and GL had a greater proportion of large soil aggregates than SF and AFL.

**Table 1.** Basic soil properties of different land patterns.

Types	Slope Position	SOC (g kg <sup>-1</sup> )	TN (g kg <sup>-1</sup> )	TP (mg kg <sup>-1</sup> )	AN (g kg <sup>-1</sup> )	AP (mg kg <sup>-1</sup> )	SWC (%)	BD (g cm <sup>-3</sup> )	pH
Sloping farmland	US	23.56 ± 5.16 Aa	0.28 ± 0.02 ABa	0.52 ± 0.06 Aa	112.63 ± 11.80 ABa	14.05 ± 3.01 ABa	17.23 ± 1.13 Aa	1.38 ± 0.06 Cb	7.17 ± 0.34 Aa
	MS	17.74 ± 2.88 Aab	0.28 ± 0.02 Aa	0.37 ± 0.06 ABa	106.76 ± 12.38 Aa	9.18 ± 2.20 Ab	19.17 ± 1.17 Aa	1.63 ± 0.07 Aa	6.77 ± 0.34 Aa
	LS	22.45 ± 1.85 Aa	0.30 ± 0.03 Aa	0.45 ± 0.05 Aa	111.49 ± 6.11 Aa	13.21 ± 2.16 Aa	15.77 ± 1.87 Aa	1.53 ± 0.05 Cab	7.05 ± 0.43 Aa
Grassland	US	25.10 ± 4.10 Aa	0.32 ± 0.02 Aa	0.52 ± 0.08 Aa	126.70 ± 14.93 Aa	9.36 ± 1.73 ABa	17.07 ± 1.09 Aa	1.73 ± 0.07 ABa	7.35 ± 0.26 Aa
	MS	19.07 ± 4.59 Aab	0.29 ± 0.03 Aa	0.53 ± 0.12 Aa	142.98 ± 9.55 Aa	9.51 ± 2.67 Aa	17.30 ± 0.97 Aa	1.79 ± 0.04 Aa	7.27 ± 0.22 Aa
	LS	20.68 ± 3.45 Aa	0.24 ± 0.01 Aa	0.33 ± 0.03 Ba	95.69 ± 6.95 Ab	4.68 ± 1.10 Bb	19.72 ± 1.87 Aa	1.92 ± 0.04 Aa	7.58 ± 0.11 Aa
Artificial forest land	US	19.44 ± 4.69 Aab	0.23 ± 0.03 Ba	0.21 ± 0.02 Bb	77.76 ± 16.49 Ba	2.77 ± 1.79 Ba	19.31 ± 1.23 Aab	1.84 ± 0.06 Da	7.72 ± 0.10 Aa
	MS	13.12 ± 4.61 Ab	0.24 ± 0.04 Aa	0.25 ± 0.02 Bab	83.11 ± 21.56 Ba	1.87 ± 0.98 Ba	15.39 ± 2.17 Ab	1.63 ± 0.13 Aa	6.33 ± 0.43 Ab
	LS	24.48 ± 9.35 Aa	0.23 ± 0.07 Aa	0.29 ± 0.03 Ba	83.92 ± 19.63 Aa	2.57 ± 0.69 Ba	20.91 ± 1.17 Aa	1.80 ± 0.05 ABa	6.96 ± 0.53 Aab
Shrubland	US	22.23 ± 5.17 Aa	0.27 ± 0.03 ABa	0.29 ± 0.03 Ba	109.63 ± 12.53 ABa	4.03 ± 0.89 Ba	17.66 ± 2.18 Aa	1.63 ± 0.07 Ba	7.56 ± 0.15 Aa
	MS	26.30 ± 7.72 Aa	0.28 ± 0.03 Aa	0.28 ± 0.03 Ba	126.54 ± 28.56 Aa	2.378 ± 0.43 Ba	19.76 ± 1.87 Aa	1.70 ± 0.06 Aa	6.78 ± 0.47 Aa
	LS	22.61 ± 6.59 Aa	0.28 ± 0.03 Aa	0.27 ± 0.02 Ba	106.54 ± 21.63 Aa	2.94 ± 0.88 Ba	18.65 ± 1.55 Aa	1.73 ± 0.04 Ba	7.25 ± 0.33 Aa

Note: Uppercase letters (A, B, C . . .) show significant differences across land use patterns on the same slope ( $p < 0.05$ ), whereas lowercase letters (a, b, c . . .) indicate significant differences between slope positions ( $p < 0.05$ ). US, upper slope; MS, middle slope; LS, lower slope. Soil organic carbon (SOC), total nitrogen (TN), total phosphorus (TP), available nitrogen (AN), available phosphorus (AP), and soil water content (SWC). Soil bulk density (BD) and soil pH (pH).

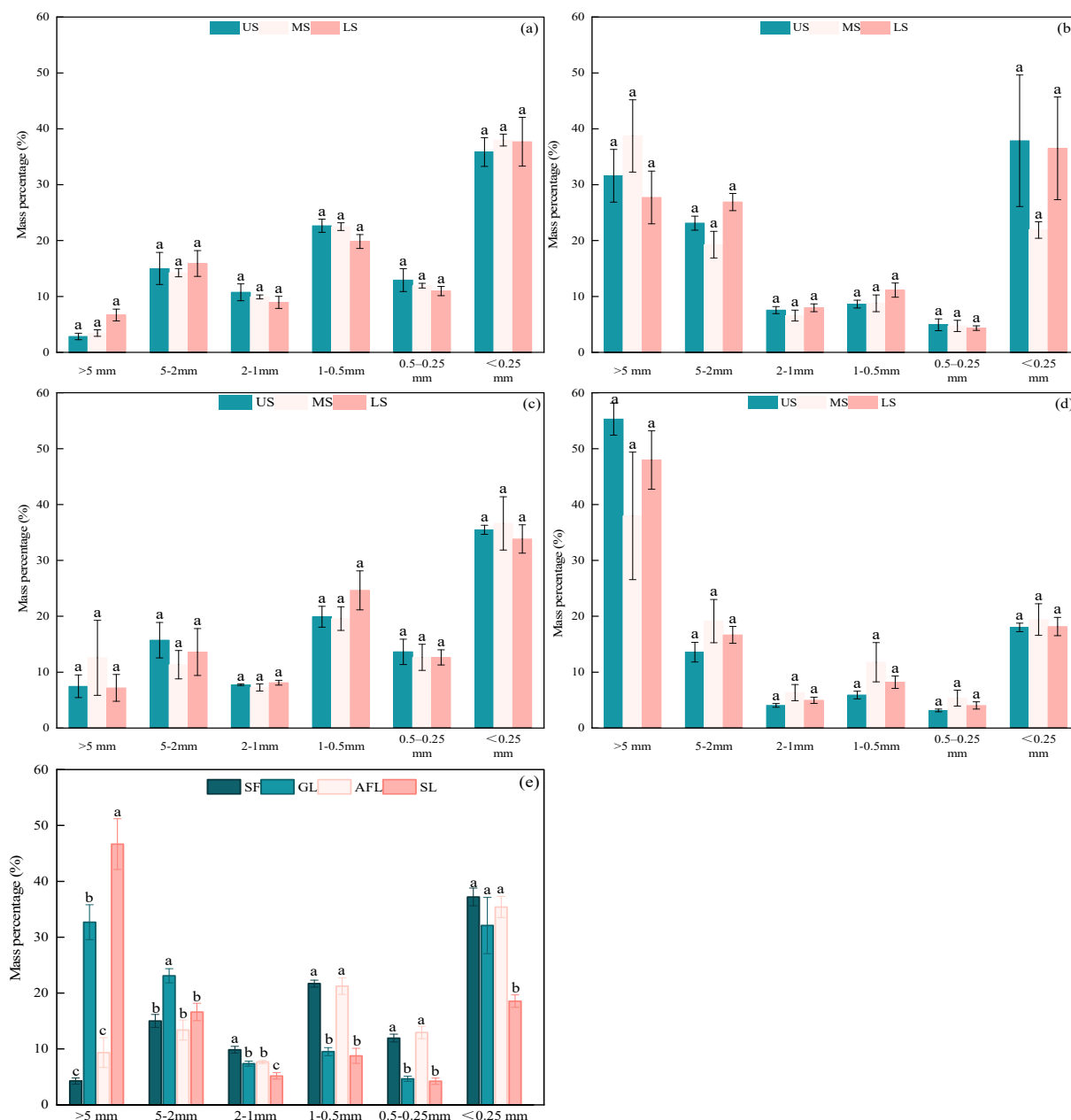


**Figure 2.** The percentage of soil water stable aggregate fractions under different land use patterns. Subfigures (a–d) represent the percentage of soil water stable aggregate fractions with different slopes in SF, GL, AFL, and SL, respectively. Subfigure (e), the percentage of soil water stable aggregate fractions with different land use patterns. Note: US, upper slope; MS, middle slope; LS, lower slope. AFL, artificial forest land; SL, shrubland; SF, sloping farmland; GL, grassland. Different lowercase letters indicate significant differences between different water stable aggregate fractions at the 0.05 level ( $p < 0.05$ ).

### 3.3. The Water Stability of Soil Aggregates under Different Land Uses

The water stability of soil aggregates under four vegetation restoration treatments is shown in Figure 3. Overall, for MWD and GMD, GL and SL were significantly higher than SF and AFL ( $p < 0.05$ ). On the contrary, for PAD, SF and AFL are significantly higher than GL and SL ( $p < 0.05$ ). For PAD, indicating a stable trend of soil aggregates, there was a descending trend from the upper slope to the lower slope. For D, there was no significant variation in D between different slope positions of four different land use patterns ( $p < 0.05$ ). For WSA<sub>0.25</sub>, the upper slope was lower than the middle slope and the lower slope. The

overall level of SL was higher. However, for SCAI, SL was lowest for WSA<sub>0.25</sub>. In general, except for the SCAI, there was no significant differences in other indices for each slope position of each land use pattern ( $p < 0.05$ ).

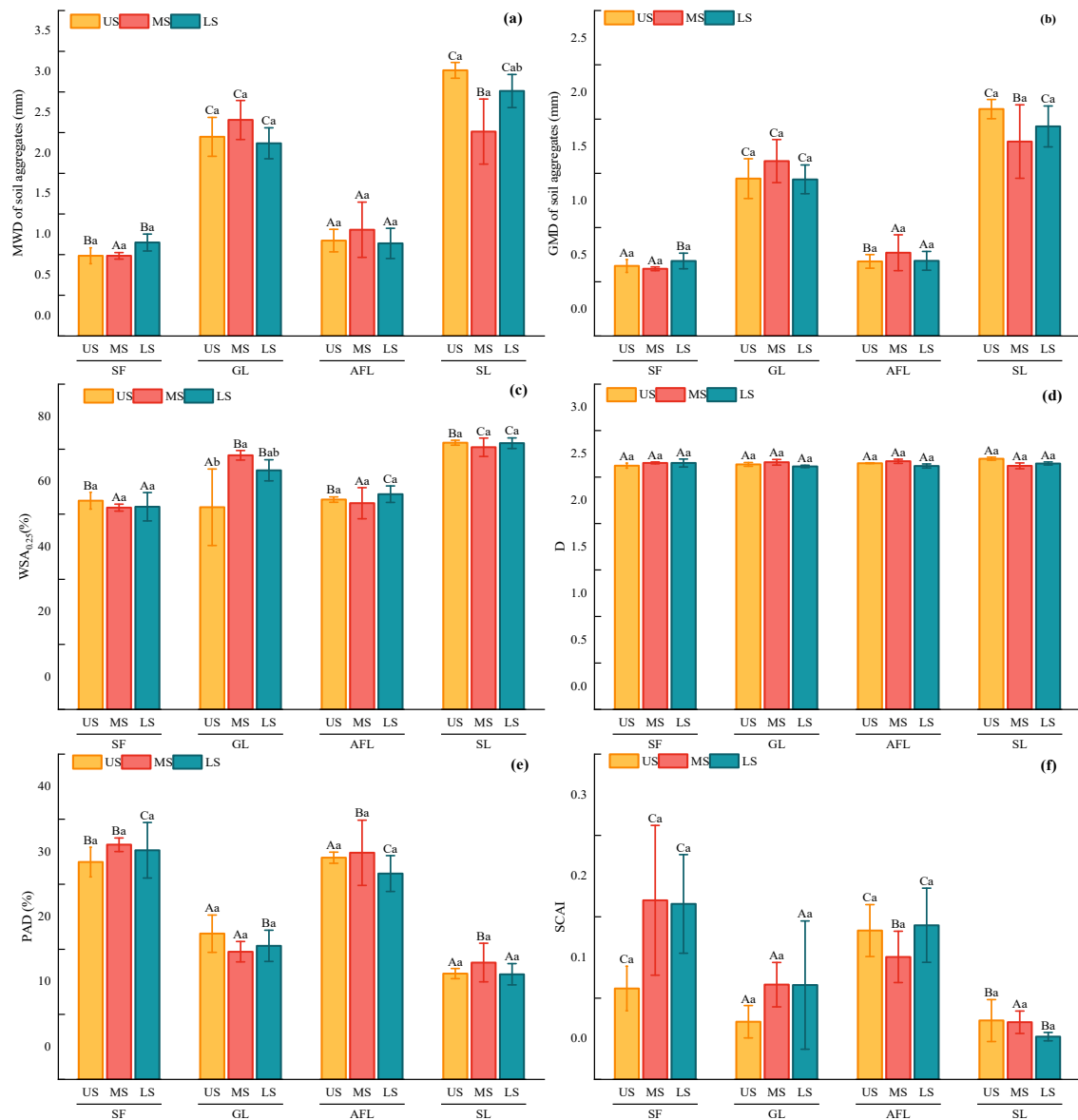


**Figure 3.** The soil stability indexes under different land patterns. Subfigures (a–f): MWD, GMD, WSA<sub>0.25</sub>, D, PAD, and SCAI in different slopes and land patterns, respectively. Note: US, upper slope; MS, middle slope; LS, lower slope. AFL, artificial forest land; SL, shrubland; SF, sloping farmland; GL, grassland. Uppercase letters (A, B, C...) show significant differences across land use patterns on the same slope ( $p < 0.05$ ), lowercase letters (a, b, c...) indicate show significant differences across between slope positions on the same land use pattern ( $p < 0.05$ ).

### 3.4. The Comparison of the Soil Erodibility

The comparison of soil erodibility is shown in Figure 4. Overall, the k-values varied from 0.144 to 0.190; GL and SL had considerably lower k-values than SF and AFL did ( $p < 0.05$ ), and there was no significant variation in different slope positions of each land use pattern. The erosion resistance of different land use patterns was GL > SL > AFL ≈ SF. This indicated that the erosion from cultivated land to soil was greater.

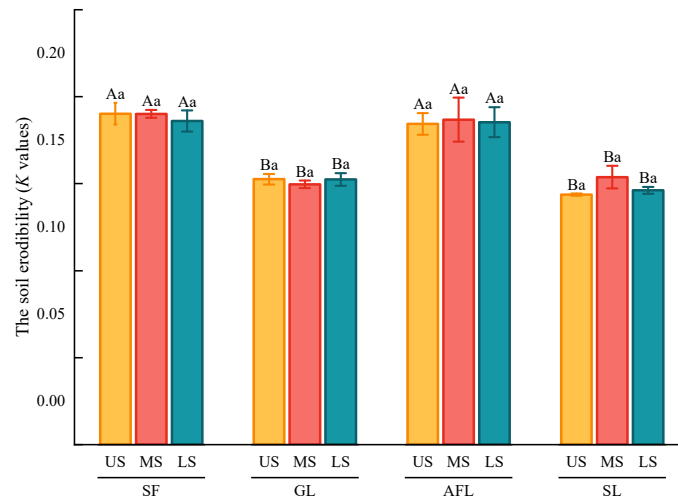


**Figure 4.** Soil erodibility (K value) under various land use patterns. Note: US, upper slope; MS, middle slope; LS, lower slope. AFL, artificial forest land; SL, shrubland; SF, sloping farmland; GL, grassland. Uppercase letters (A, B, C...) show significant differences across land use patterns on the same slope ( $p < 0.05$ ), lowercase letters (a, b, c...) indicate show significant differences across between slope positions on the same land use pattern ( $p < 0.05$ ).

### 3.5. Correlation between Soil Properties and Soil Water Stable Aggregate Fraction

According to the correlation analysis (Figure 5), overall, BD was significantly positively correlated with >5 mm, MWD, GMD and SCAI, and significantly negative correlated with 2–1 mm, 1–0.5 mm, 0.5–0.25 mm and K. PH had a positive correlation with >5 mm, 5–2 mm, MWD, GMD and  $WSA_{0.25}$  and had a negative correlation with 0.5–1 mm, 0.25–0.5 mm, PAD and K. AP was positively correlated with 2–1 mm, 1–0.5 mm, PAD and K and had a negative correlation with >5 mm, MWD, GMD,  $WSA_{0.25}$  and SCAI. AN was significantly positively correlated with MWD, GMD and  $WSA_{0.25}$  and significantly negatively correlated with <0.25 mm, PAD and K. TN, TP and SOC were significantly negatively correlated with SCAI ( $p < 0.05$ ).

### 3.6. Comprehensive Evaluation of Soil Aggregate Stability

The four PCAs explained 72.511% of the total variance, satisfying the principal component (PC) requirement (Table 2). The factor loading matrix data for each index were divided by the square root of the PC eigenvalues to calculate the coefficients for the two PCs. The obtained coefficients were multiplied by the normalised data to obtain the formula for each PC as follows:

$$F_1 = -0.134X_1 - 0.019X_2 + 0.033X_3 - 0.047X_4 + 0.066X_5 + 0.019X_6 - 0.042X_7 - 0.013X_8 + 0.244X_9 + 0.236X_{10} + 0.189X_{11} - 0.004X_{12} - 0.245X_{13} + 0.196X_{14}$$

$$F_2 = 0.21X_1 + 0.029X_2 + 0.204X_3 + 0.338X_4 + 0.212X_5 + 0.245X_6 + 0.06X_7 + 0.087X_8 + 0.01X_9 + 0.031X_{10} + 0.012X_{11} + 0.056X_{12} + 0.012X_{13} - 0.237X_{14}$$

$$F_3 = 0.548X_1 + 0.397X_2 + 0.176X_3 + 0.188X_4 - 0.092X_5 - 0.034X_6 - 0.282X_7 - 0.269X_8 - 0.043X_9 - 0.019X_{10} - 0.015X_{11} + 0.012X_{12} + 0.054X_{13} - 0.17X_{14}$$

$$F_4 = 0.003X_1 + 0.059X_2 - 0.105X_3 + 0.077X_4 + 0.031X_5 + 0.061X_6 + 0.12X_7 + 0.017X_8 + 0.158X_9 + 0.179X_{10} - 0.195X_{11} + 0.825X_{12} + 0.177X_{13} + 0.085X_{14}$$

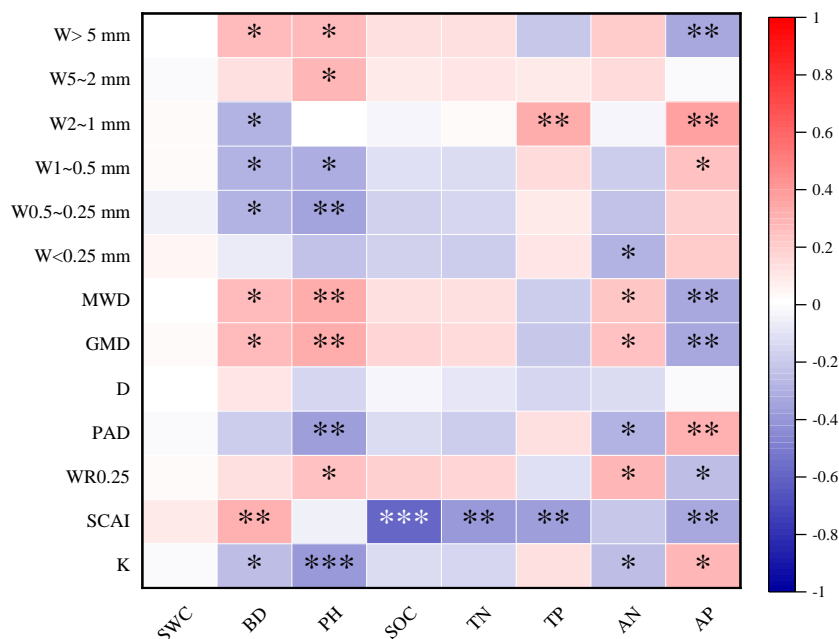


**Figure 5.** The correlations between soil properties and soil water stable aggregate fractions, soil stability indexes and K values. Note: the mean correlation coefficients shown by \*, \*\*, and \*\*\* are significant at the 0.05, 0.01 and 0.001 levels, respectively. SWC, soil water content; BD, soil bulk density; pH, soil pH; SOC, soil organic carbon; TN, total nitrogen; TP, total phosphorus; AN, available nitrogen; AP, available phosphorus; W > 5 mm, % of water stable aggregates > 5 mm; W5-2 mm, % of water stable aggregates 5–2 mm; W2-1 mm, % of water stable aggregates 2–1 mm; W1-5 mm, % of water stable aggregates 1–0.5 mm; W0.5-0.25 mm, % of water stable aggregates 0.5–0.25 mm; W < 0.25 mm, % of water stable aggregates < 0.25 mm; GMD, geometric mean diameter; MWD, mean weight diameter; PAD, percentage of aggregate destruction; D, fractal dimension; WR0.25, WSA<sub>0.25</sub> > 0.25 mm aggregate specific gravity; SCAI, SOC cementing agent index; K, soil erodibility.

**Table 2.** Loading matrix and standardized coefficients based on PC analysis.

Indexes	PCs				Coefficient Matrix			
	PC <sub>1</sub>	PC <sub>2</sub>	PC <sub>3</sub>	PC <sub>4</sub>	1	2	3	4
X <sub>1</sub>	0.096	−0.124	0.662	0.239	−0.134	0.210	0.548	0.003
X <sub>2</sub>	0.365	−0.502	0.385	0.191	−0.019	0.029	0.397	0.059
X <sub>3</sub>	0.369	0.470	0.291	−0.004	0.033	0.204	0.179	−0.105
X <sub>4</sub>	0.081	0.795	0.301	0.24	−0.047	0.338	0.188	0.077
X <sub>5</sub>	0.208	0.826	−0.039	0.061	0.066	0.212	−0.092	0.031
X <sub>6</sub>	0.089	0.827	0.033	0.123	0.019	0.245	−0.034	0.061
X <sub>7</sub>	−0.467	0.534	−0.293	0.066	−0.042	0.060	−0.282	0.120
X <sub>8</sub>	−0.331	0.656	−0.235	−0.036	−0.013	0.087	−0.269	0.017
X <sub>9</sub>	0.947	0.079	−0.172	0.136	0.244	0.010	−0.043	0.158
X <sub>10</sub>	0.945	0.100	−0.146	0.172	0.236	0.031	−0.019	0.179
X <sub>11</sub>	0.754	0.193	0.014	−0.229	0.189	0.012	−0.015	−0.195
X <sub>12</sub>	0.010	−0.215	−0.300	0.906	−0.004	0.056	0.012	0.825
X <sub>13</sub>	−0.933	−0.174	0.056	0.234	−0.245	0.012	0.054	0.177
X <sub>14</sub>	0.564	−0.527	−0.352	−0.046	0.196	−0.237	−0.17	0.085
Eigenvalue	2.697	2.938	0.205	2.053				
Variance (%)	39.500	31.387	17.319	11.794				
Cumulative variance (%)	28.642	51.401	63.958	72.511				

Note: PC, Principal component; X<sub>1</sub>, RWC; X<sub>2</sub>, BD; X<sub>3</sub>, pH; X<sub>4</sub>, SOC; X<sub>5</sub>, AN; X<sub>6</sub>, TN; X<sub>7</sub>, AP; X<sub>8</sub>, TP; X<sub>9</sub>, MWD; X<sub>10</sub>, GMD; X<sub>11</sub>, WSA<sub>0.25</sub>; X<sub>12</sub>, D; X<sub>13</sub>, PAD; X<sub>14</sub>, SCAI.

The combined PC score for resistance to soil erosion (composite score) was calculated by dividing the contribution of each PC by the total contribution of PCs 1 to 4 as weights, giving the following equation:

$$F = 0.395F_1 + 0.314F_2 + 0.173F_3 + 0.118F_4$$

The comprehensive evaluation of soil aggregate stability and soil erosion resistance are shown in Figure 6. Our results showed that for the upper slope and the low slope, SL got the greatest comprehensive score, and SF had the lowest comprehensive score (Figure 6a,c). For the medium slope, SL had the highest comprehensive score, and AFL had the lowest comprehensive score (Figure 6b). Overall, SL > GL > AFL > SF in the comprehensive score of all land use patterns (Figure 6d).

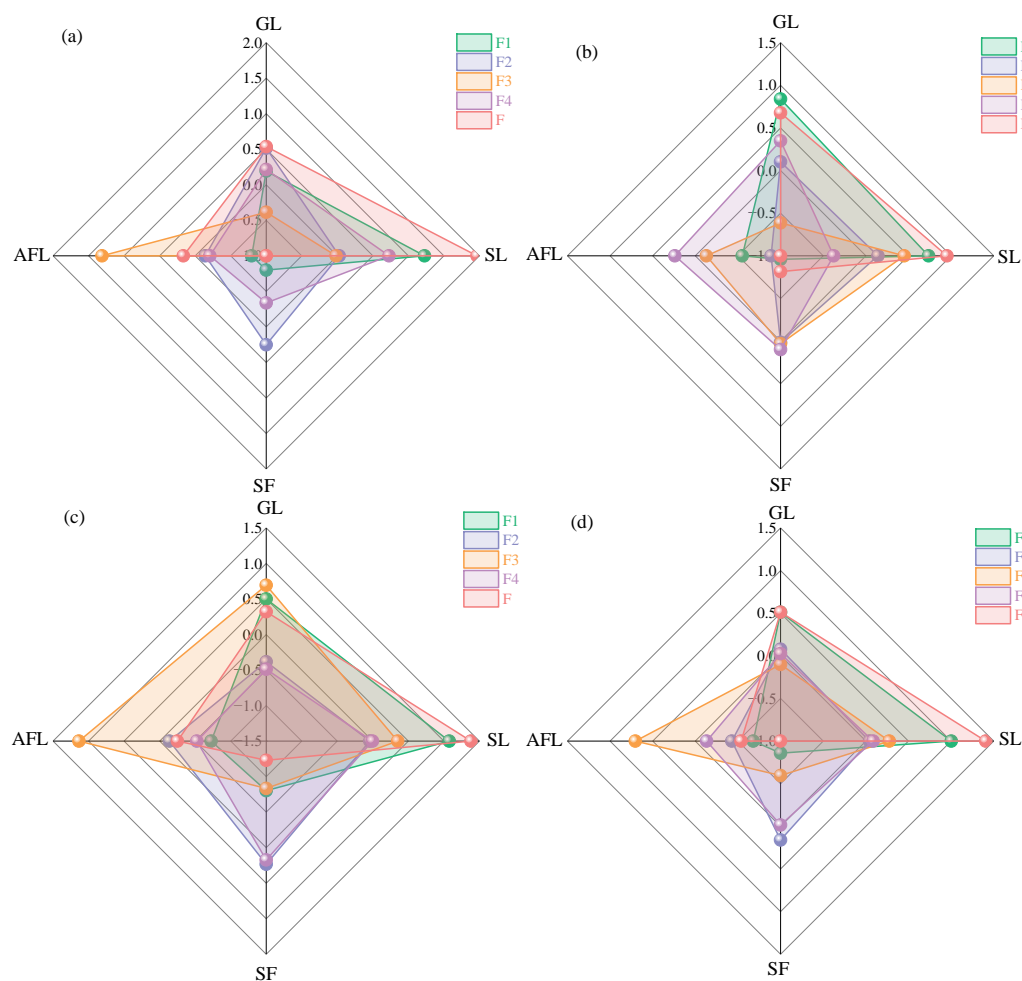


**Figure 6.** Comprehensive scores of different land patterns. Subfigures (a–c) show comprehensive scores for upper, middle, and lower slopes, respectively, and (d) shows scores for different land patterns. Note: US, upper slope; MS, middle slope; LS, lower slope. AFL, artificial forest land; SL, shrubland; SF, sloping farmland; GL, grassland.

## 4. Discussion

### 4.1. Influence of Different Land Use Patterns on the Particle Size Distribution of Aggregates

The distribution of soil aggregate sizes responds rapidly to land use changes and may act as an indication of soil quality [37]. The results we obtained indicate that the distribution of soil aggregate mass percentage is mainly concentrated in >0.25 mm for water stable aggregates of all land use patterns. This result was also reported by Xiao et al. (2017) and Liao et al. (2016) [38,39], who also conducted their studies in karst areas. Different land use patterns could cause changes

in soil agglomerate dynamics, and Gelaw et al. (2015) [40] reported that after conversion of agricultural land to *Faidherbia albida* plantations, the proportion of soil macroaggregates at 0–20 cm soil depth increased by 68.2%, while a percentage of microaggregates decreased by 48.0%, indicating that macroaggregates and microaggregates have different sensitivities to land use pattern. Dou et al. (2020) and Zhou et al. (2022) [9,18] found that soil aggregates < 0.25 mm were dominant. This differs from the results presented here, which may be attributed to variations in soil texture, vegetation type and soil depth across the Loess Plateau. The magnitude of change in aggregates of 5–2 mm, 2–1 mm and 0.5–0.25 mm is relatively stable compared to >5 mm, due to changes in land use that generally result in the destruction or formation of soil aggregates [41], while vulnerability to water erosion is more likely to destroy soil aggregates of >5 mm [9,42]. For <0.25 mm, we found that SF was more degraded than other land types, with a mass fraction of microaggregates as high as 37.21%. This may be attributed to the greater disturbance of the overlying vegetation on sloping land, which is degraded by severe water erosion and the ease with which large aggregates are broken down into smaller aggregates, which is in agreement with the findings of this and early research [9,43].

In addition, GL and SL have more large soil aggregates compared to SF and AFL. This result could be explained by the fact that a large number of *Lolium perenne* L., *Medicago sativa*, *Coriaria nepalensis* and other plants are planted in SL and GL, and their above-ground biomass is higher, resulting in more roots or litter, thus promoting the formation of large aggregates. Sheng et al. (2019) [41] also showed that in grasslands, the continuous input of plant residues promotes the aggregation of soil particles, leading to the formation of microaggregates into large aggregates, thereby increasing large aggregates and decreasing small aggregates. In other words, an increase in the mass fraction of large aggregates leads to a corresponding increase in aggregate stability, which facilitates the maintenance and accumulation of nutrients such as soil SOC; conversely, an increase in soil organic carbon promotes the formation of macroaggregates.

#### 4.2. Response of the Stability of Soil Aggregates to Different Land Use Patterns

Land use affects soil aggregate particle size distribution and stability [44]. The stability of soil aggregates is significant for the stability of soil aggregates under land use change and is an index for assessing soil quality [45]. The  $WSA_{0.25}$ , MWD and GMD are key indices for evaluating the stability of soil aggregates. The higher their values, the better the stability [9,46]. In our study,  $WSA_{0.25}$ , MWD and GMD of soil aggregates were greater in SL and GL than in SF and AFL, especially in SL. *Pyracantha fortuneana* and *Coriaria nepalensis*, both of which have dense root systems. The stability of large aggregates may be protected by their strong soil and water conserving capacity. In addition to other soil and environmental factors, the kind of land use or land cover have a significant impact on soil aggregate stability [17]. Liu et al. (2020) [26] indicated that soil aggregate stability could respond rapidly to changes in land use, and results also showed that soil aggregate stability was significantly lower in karst farmland than in abandoned farmland and primary vegetation. Additionally, earlier studies have also indicated that cultivated land has substantially less soil aggregate stability than other land uses [14]. Tilled soils are more prone to water erosion than shrubland and grassland, leading to a significant reduction in the stability of soil aggregates, whereas no-tillage can enhance macroaggregate stability [47]. Therefore, in comparison to tilled land, SL can protect soil aggregate integrity and improve soil aggregate stability.

Fractal dimension (D), as well as being one measure of soil stability, is also used as a substitute indication to describe the processes leading to desertification [48]. PAD is a crucial indication of aggregate stability and measures the degree of dispersion between soil aggregates under water erosion. Soil aggregates have a decreasing value as they become more stable. And SCAI was used to show the relationship between SOC content and soil aggregate stability [36]. The lower the value of SCAI, the higher the stability of the soil aggregates. The results showed that the PAD of SL and GL are lower, but there was no significant difference in D between the different land use patterns. SL and GL crops

can improve soil water stability and reduce aggregate degradation. The change trend of SCAI shows that SL surface soil organic matter is higher, and organic carbon has a greater consolidating effect on soil aggregates [36], which promotes the formation of large aggregates. In addition, except for SCAI, there is no significant difference in each index of different slope positions. The effect of slope position is small, probably because the elevation of different slope positions of each land use pattern is not large in the study area.

#### 4.3. Effects of the Pattern of Land Use on the Soil Erodibility

Soil erodibility K-value can reflect soil physical structure stability and is also an important parameter to evaluate soil conservation effect [9,24,49]. The soil is less prone to erosion, the lower the K value. Our results show that the erosion resistance of the different land use patterns is in the order  $GL > SL > AFL \approx SF$ . This is in line with those of previous studies [9,24], which indicate that the soil erosion degree of scrubland is lighter for all land use patterns. In karst areas, the EPIC model is often used to assess soil erodibility. For example, Luo et al. (2022) [50] utilised the EPIC model to evaluate soil erodibility in karst areas, with an evaluation range of 0.0436–0.0520. The K value of vegetable fields and terraces is the highest, while that of natural mixed forests is the lowest. The limitation of this method, however, is that it does not take into account the permeability of the soil associated with large aggregates [26]. In addition, calcium in calcareous soils could have a serious impact on aggregate formation and soil structure and hence, on soil erosion [26,51].

Research has shown that soil erodibility is influenced not only by soil properties [52] but also by land use patterns and soil management practices [45]. Globally, soil erosion is lower in scrubland and higher in cropland [53], with the worst soil erosion occurring on bare land [54]. According to Wang et al. (2019) [9], agricultural land has significantly greater soil erodibility than forest, grassland, arbour forest and shrub land. On the one hand, the increase in vegetation also increased soil resistance, resulting in a significant decrease in the ability of surface runoff to strip soil [55]. On the other hand, the increase in aboveground biomass after the conversion of sloping farmland to land covered with different vegetation increased organic matter, improved soil fertilities and promoted the formation of new and richer aggregates [56,57], which increased the stability of soil aggregates and thereby increased soil resistance to erosion. Therefore, improving the stability of soil aggregates and reducing soil susceptibility to erosion can be achieved through vegetation measures [58].

#### 4.4. Correlation between Soil Aggregate Stability Index and Soil Properties

Soil aggregate stability and soil erodibility are significant indications of soil degradation [6,59]. In this work, we noted that the negative correlation between BD and K-factor indicates that increasing soil bulk density reduces soil macropores, which in turn reduces the production of large aggregates. BD had a negative effect on the percentage of soil aggregates < 2 mm. To some extent, BD inhibits plant root growth and reduces soil microbial activity, thereby limiting aggregate formation [18] and reducing soil permeability and erosion resistance. The negative correlation between AP and >5 mm indicates that the larger the particle size of soil aggregates, the smaller the specific surface area and the weaker the adsorption capacity of nutrients available in the soil [60]. SOC, TN and TP had significantly negative correlations with SCAI. This indicates that increased soil stability leads to higher C, N and P nutrient contents, lower organic matter decomposition rates and higher amounts of organic matter that are kept in the soil, all of which are favourable for the buildup of soil organic matter. Organic matter is a crucial binder for forming soil water-stable macroaggregates, which can promote macroaggregate formation [18]. Therefore, the destruction of aggregates is reduced, which plays a role in forming and protecting aggregates, resulting in reduced soil erodibility. In addition, increasing the proportion of large aggregation in soils has been identified as a key breakthrough for improving soil fertility and soil environmental quality [61].

#### 4.5. The Limit of Study

In this study, the effects of four land use patterns on the stability and erodibility of soil aggregates in a typical karst plateau wetland ecosystem were evaluated. This study adds to our understanding of soil aggregate stability and erodibility under different land use patterns in karst plateau wetland ecosystems. Before drawing conclusions, however, some limitations should be highlighted. Firstly, research should be further extended to other depths [9,18,26], as this study is limited to the surface layer of soil. Second, the results of our research show that, under four land use patterns, the physical and chemical characteristics of the soil and the stability of the aggregates at the three slope locations did not significantly differ from one another. This might be because there was no significant difference in soil properties in geospatial locations, as the elevation of the slope positions in the study area was not very different. Finally, small catchment sampling is limited. In future studies, more sampling plots should be considered, more samples should be extended and more land use patterns should be combined to obtain accurate, reliable information on soil aggregate stability and erodibility.

#### 5. Conclusions

The effects of different types of land use on the stability and erodibility of soil aggregates were studied in a typical wetland ecosystem of the Guizhou karst plateau. The results indicated that soil aggregates were predominantly large aggregates > 0.25 mm; soil aggregate stability was highest under SL, followed by GL and lowest under SF. Furthermore, under different slopes of the same land use, there was no obvious difference in the stability of soil aggregates. Overall, land use significantly affects soil aggregate stability and erodibility, particularly for SL. This study helps to better understand the stability of soil aggregates under various land use types in the karst plateau wetland ecosystem and to develop control strategies for soil erosion and improve soil qualities.

**Supplementary Materials:** The following supporting information can be downloaded at: <https://www.mdpi.com/article/10.3390/f15040599/s1>, Table S1: Basic information about research plots.

**Author Contributions:** Conceptualization, L.C. and X.P.; methodology, X.P.; software, L.C.; validation, Q.D.; formal analysis, L.C.; writing—original draft preparation, L.C.; writing—review and editing, X.P.; visualization, L.C.; funding acquisition, X.P. All authors have read and agreed to the published version of the manuscript.

**Funding:** This research was funded by the Guizhou Provincial Key Technology R&D Program (QKHZC [2023] YB104), the National Natural Science Foundation of China (NO. 42267054, 42007067), the Guizhou Provincial Basic Research Program (Natural Science) (QKHJC [2020] 1Y176).

**Data Availability Statement:** The data presented in this study are available upon request from the corresponding author.

**Conflicts of Interest:** The authors declare no conflicts of interest.

#### References

1. Fluet-Chouinard, E.; Stocker, B.D.; Zhang, Z.; Malhotra, A.; Melton, J.R.; Poulter, B.; Kaplan, J.O.; Goldewijk, K.K.; Siebert, S.; Minayeva, T.; et al. Extensive Global Wetland Loss over the Past Three Centuries. *Nature* **2023**, *614*, 281–286. [[CrossRef](#)] [[PubMed](#)]
2. Borrelli, P.; Robinson, D.A.; Fleischer, L.R.; Lugato, E.; Ballabio, C.; Alewell, C.; Meusburger, K.; Modugno, S.; Schütt, B.; Ferro, V.; et al. An Assessment of the Global Impact of 21st Century Land Use Change on Soil Erosion. *Nat. Commun.* **2017**, *8*, 2013. [[CrossRef](#)] [[PubMed](#)]
3. Devátý, J.; Dostál, T.; Hösl, R.; Krása, J.; Strauss, P. Effects of Historical Land Use and Land Pattern Changes on Soil Erosion—Case Studies from Lower Austria and Central Bohemia. *Land Use Policy* **2019**, *82*, 674–685. [[CrossRef](#)]
4. Cao, Z.; Zhang, K.; He, J.; Yang, Z.; Zhou, Z. Linking Rocky Desertification to Soil Erosion by Investigating Changes in Soil Magnetic Susceptibility Profiles on Karst Slopes. *Geoderma* **2021**, *389*, 114949. [[CrossRef](#)]
5. Zhang, Z.; Wu, X.; Zhang, J.; Huang, X. Distribution and Migration Characteristics of Microplastics in Farmland Soils, Surface Water and Sediments in Caohai Lake, Southwestern Plateau of China. *J. Cleaner Prod.* **2022**, *366*, 132912. [[CrossRef](#)]
6. Ye, L.; Tan, W.; Fang, L.; Ji, L.; Deng, H. Spatial Analysis of Soil Aggregate Stability in a Small Catchment of the Loess Plateau, China: I. Spatial Variability. *Soil Tillage Res.* **2018**, *179*, 71–81. [[CrossRef](#)]

7. Li, H.; Zhu, H.; Qiu, L.; Wei, X.; Liu, B.; Shao, M. Response of Soil OC, N and P to Land-Use Change and Erosion in the Black Soil Region of the Northeast China. *Agric. Ecosyst. Environ.* **2020**, *302*, 107081. [[CrossRef](#)]
8. Six, J.; Paustian, K. Aggregate-Associated Soil Organic Matter as an Ecosystem Property and a Measurement Tool. *Soil Biol. Biochem.* **2014**, *68*, A4–A9. [[CrossRef](#)]
9. Dou, Y.; Yang, Y.; An, S.; Zhu, Z. Effects of Different Vegetation Restoration Measures on Soil Aggregate Stability and Erodibility on the Loess Plateau, China. *Catena* **2020**, *185*, 104294. [[CrossRef](#)]
10. Mounirou, L.A.; Yonaba, R.; Tazen, F.; Ayele, G.T.; Yaseen, Z.M.; Karambiri, H.; Yacouba, H. Soil Erosion across Scales: Assessing Its Sources of Variation in Sahelian Landscapes under Semi-Arid Climate. *Land* **2022**, *11*, 2302. [[CrossRef](#)]
11. Caravaca, F.; Lax, A.; Albaladejo, J. Soil Aggregate Stability and Organic Matter in Clay and Fine Silt Fractions in Urban Refuse-amended Semiarid Soils. *Soil Sci. Soc. Am. J.* **2001**, *65*, 1235–1238. [[CrossRef](#)]
12. Zuo, L.; Zhang, Z.; Carlson, K.M.; MacDonald, G.K.; Brauman, K.A.; Liu, Y.; Zhang, W.; Zhang, H.; Wu, W.; Zhao, X.; et al. Progress towards Sustainable Intensification in China Challenged by Land-Use Change. *Nat. Sustain.* **2018**, *1*, 304–313. [[CrossRef](#)]
13. Schweizer, S.A.; Fischer, H.; Häring, V.; Stahr, K. Soil Structure Breakdown Following Land Use Change from Forest to Maize in Northwest Vietnam. *Soil Tillage Res.* **2017**, *166*, 10–17. [[CrossRef](#)]
14. Delelegn, Y.T.; Purahong, W.; Blazevic, A.; Yitaferu, B.; Wubet, T.; Göransson, H.; Godbold, D.L. Changes in Land Use Alter Soil Quality and Aggregate Stability in the Highlands of Northern Ethiopia. *Sci. Rep.* **2017**, *7*, 13602. [[CrossRef](#)] [[PubMed](#)]
15. Melese, T.; Senamaw, A.; Belay, T.; Bayable, G. The Spatiotemporal Dynamics of Land Use Land Cover Change, and Its Impact on Soil Erosion in Tagaw Watershed, Blue Nile Basin, Ethiopia. *Glob. Chall.* **2021**, *5*, 2000109. [[CrossRef](#)]
16. Behrends Kraemer, F.; Hallett, P.D.; Morrás, H.; Garibaldi, L.; Cosentino, D.; Duval, M.; Galantini, J. Soil Stabilisation by Water Repellency under No-till Management for Soils with Contrasting Mineralogy and Carbon Quality. *Geoderma* **2019**, *355*, 113902. [[CrossRef](#)]
17. Dorji, T.; Field, D.J.; Odeh, I.O.A. Soil Aggregate Stability and Aggregate-associated Organic Carbon under Different Land Use or Land Cover Types. *Soil Use Manag.* **2020**, *36*, 308–319. [[CrossRef](#)]
18. Zhou, Y.; Ma, H.; Xie, Y.; Lu, Q.; Shen, Y.; Ma, J. Response of Soil Aggregate Stability and Erodibility to Different Treatments on Typical Steppe in the Loess Plateau, China. *Restor. Ecol.* **2022**, *30*, e13593. [[CrossRef](#)]
19. Zhu, G.; Deng, L.; Shanguan, Z. Effects of Soil Aggregate Stability on Soil N Following Land Use Changes under Erodible Environment. *Agric. Ecosyst. Environ.* **2018**, *262*, 18–28. [[CrossRef](#)]
20. Zhong, Z.; Han, X.; Xu, Y.; Zhang, W.; Fu, S.; Liu, W.; Ren, C.; Yang, G.; Ren, G. Effects of Land Use Change on Organic Carbon Dynamics Associated with Soil Aggregate Fractions on the Loess Plateau, China. *Land Degrad. Dev.* **2019**, *30*, 1070–1082. [[CrossRef](#)]
21. Lan, J. Changes of Soil Aggregate Stability and Erodibility After Cropland Conversion in Degraded Karst Region. *J. Soil Sci. Plant Nutr.* **2021**, *21*, 3333–3345. [[CrossRef](#)]
22. Tan, Z.; Wan, F.; Zhang, B. Evaluation of Soil Antierodibility of Different Forests in Volcanic Hilly Land of Xuyi County. *Res. Soil Water Conserv.* **2015**, *22*, 7–11. (in Chinese). [[CrossRef](#)]
23. Madenoglu, S.; Atalay, F.; Erpul, G. Uncertainty Assessment of Soil Erodibility by Direct Sequential Gaussian Simulation (DSIM) in Semiarid Land Uses. *Soil Tillage Res.* **2020**, *204*, 104731. [[CrossRef](#)]
24. Wang, H.; Zhang, G.; Li, N.; Zhang, B.; Yang, H. Variation in Soil Erodibility under Five Typical Land Uses in a Small Watershed on the Loess Plateau, China. *Catena* **2019**, *174*, 24–35. [[CrossRef](#)]
25. Chen, S.; Zhang, G.; Zhu, P.; Wang, C.; Wan, Y. Impact of Land Use Type on Soil Erodibility in a Small Watershed of Rolling Hill Northeast China. *Soil Tillage Res.* **2023**, *227*, 105597. [[CrossRef](#)]
26. Liu, M.; Han, G. Assessing Soil Degradation under Land-Use Change: Insight from Soil Erosion and Soil Aggregate Stability in a Small Karst Catchment in Southwest China. *PeerJ* **2020**, *8*, e8908. [[CrossRef](#)] [[PubMed](#)]
27. Zhang, Y.; Jin, R.; Zhu, W.; Zhang, D.; Zhang, X. Impacts of Land Use Changes on Wetland Ecosystem Services in the Tumen River Basin. *Sustainability* **2020**, *12*, 9821. [[CrossRef](#)]
28. Zhang, Z.; Lin, S.; Zhang, Q.; Guo, Y.; Lin, C. The Distribution Characteristics of Soil Carbon, Nitrogen and Phosphorus Under Different Land Use Patterns in Caohai Plateau Wetland. *J. Soil Water Conserv.* **2013**, *27*, 199–204. (In Chinese) [[CrossRef](#)]
29. Lin, S.; Zhang, Q.; Guo, Y.; Ouyang, Y.; Lin, C. Pollution Characteristics and Potential Ecological Risk Assessment of Heavy Metals in Sediments of Caohai in Guizhou Province, China. *J. Agro-Environ. Sci.* **2012**, *31*, 2236–2241. (In Chinese)
30. Yang, H.; Chen, J.; Liu, W.; Wang, J.; Li, J.; Ji, Y.; Chen, Y. Distribution Characteristics and Controlling Factors of Total Organic Carbon, Total Nitrogen, and Total Phosphorus in Sediments of Caohai Lake, China. *Earth Environ.* **2016**, *44*, 297–303. (in Chinese). [[CrossRef](#)]
31. Xia, P.; Ma, L.; Sun, R.; Yang, Y.; Tang, X.; Yan, D.; Lin, T.; Zhang, Y.; Yi, Y. Evaluation of Potential Ecological Risk, Possible Sources and Controlling Factors of Heavy Metals in Surface Sediment of Caohai Wetland, China. *Sci. Total Environ.* **2020**, *740*, 140231. [[CrossRef](#)] [[PubMed](#)]
32. Bastola, S.; Dialynas, Y.G.; Bras, R.L.; Noto, L.V.; Istanbuluoglu, E. The Role of Vegetation on Gully Erosion Stabilization at a Severely Degraded Landscape: A Case Study from Calhoun Experimental Critical Zone Observatory. *Geomorphology* **2018**, *308*, 25–39. [[CrossRef](#)]

33. Zhao, J.; Chen, S.; Hu, R.; Li, Y. Aggregate Stability and Size Distribution of Red Soils under Different Land Uses Integrally Regulated by Soil Organic Matter, and Iron and Aluminum Oxides. *Soil Tillage Res.* **2017**, *167*, 73–79. [[CrossRef](#)]
34. Institute of Soil Science, Chinese Academy of Sciences. *Soil Chemical and Physical Analysis*; Shanghai Science and Technology Press: Shanghai, China, 1978.
35. Bremner, J.M.; Keeney, D.R. Determination and Isotope-Ratio Analysis of Different Forms of Nitrogen in Soils: 3. Exchangeable Ammonium, Nitrate, and Nitrite by Extraction-Distillation Methods. *Soil Sci. Soc. Am. J.* **1966**, *30*, 577–582. [[CrossRef](#)]
36. Jiang, Y.; Zheng, F.; Wen, L.; Shen, H. Effects of Sheet and Rill Erosion on Soil Aggregates and Organic Carbon Losses for a Mollisol Hillslope under Rainfall Simulation. *J. Soils Sediments* **2019**, *19*, 467–477. [[CrossRef](#)]
37. Nie, M.; Pendall, E.; Bell, C.; Wallenstein, M.D. Soil Aggregate Size Distribution Mediates Microbial Climate Change Feedbacks. *Soil Biol. Biochem.* **2014**, *68*, 357–365. [[CrossRef](#)]
38. Xiao, S.; Zhang, W.; Ye, Y.; Zhao, J.; Wang, K. Soil Aggregate Mediates the Impacts of Land Uses on Organic Carbon, Total Nitrogen, and Microbial Activity in a Karst Ecosystem. *Sci. Rep.* **2017**, *7*, 41402. [[CrossRef](#)] [[PubMed](#)]
39. Liao, H.; Long, J.; Li, J. Conversion of Cropland to Chinese Prickly Ash Orchard Affects Soil Organic Carbon Dynamics in a Karst Region of Southwest China. *Nutr. Cycling Agroecosyst.* **2016**, *104*, 15–23. [[CrossRef](#)]
40. Gelaw, A.M.; Singh, B.R.; Lal, R. Organic Carbon and Nitrogen Associated with Soil Aggregates and Particle Sizes Under Different Land Uses in Tigray, Northern Ethiopia. *Land Degrad. Dev.* **2015**, *26*, 690–700. [[CrossRef](#)]
41. Sheng, M.; Han, X.; Zhang, Y.; Long, J.; Li, N. 31-Year Contrasting Agricultural Managements Affect the Distribution of Organic Carbon in Aggregate-Sized Fractions of a Mollisol. *Sci. Rep.* **2020**, *10*, 9041. [[CrossRef](#)]
42. Ayoubi, S.; Mokhtari Karchegani, P.; Mosaddeghi, M.R.; Honarjoo, N. Soil Aggregation and Organic Carbon as Affected by Topography and Land Use Change in Western Iran. *Soil Tillage Res.* **2012**, *121*, 18–26. [[CrossRef](#)]
43. Cambardella, C.A.; Elliott, E.T. Carbon and Nitrogen Distribution in Aggregates from Cultivated and Native Grassland Soils. *Soil Sci. Soc. Am. J.* **1993**, *57*, 1071–1076. [[CrossRef](#)]
44. Hu, F.; Xu, C.; Li, H.; Li, S.; Yu, Z.; Li, Y.; He, X. Particles Interaction Forces and Their Effects on Soil Aggregates Breakdown. *Soil Tillage Res.* **2015**, *147*, 1–9. [[CrossRef](#)]
45. Zhu, G.; Tang, Z.; Shangguan, Z.; Peng, C.; Deng, L. Factors Affecting the Spatial and Temporal Variations in Soil Erodibility of China. *J. Geophys. Res. Earth Surf.* **2019**, *124*, 737–749. [[CrossRef](#)]
46. Padbhushan, R.; Rakshit, R.; Das, A.; Sharma, R.P. Effects of Various Organic Amendments on Organic Carbon Pools and Water Stable Aggregates under a Scented Rice–Potato–Onion Cropping System. *Paddy Water Environ.* **2016**, *14*, 481–489. [[CrossRef](#)]
47. Celik, I. Land-Use Effects on Organic Matter and Physical Properties of Soil in a Southern Mediterranean Highland of Turkey. *Soil Tillage Res.* **2005**, *83*, 270–277. [[CrossRef](#)]
48. Gao, G.-L.; Ding, G.-D.; Zhao, Y.-Y.; Wu, B.; Zhang, Y.-Q.; Qin, S.-G.; Bao, Y.-F.; Yu, M.-H.; Liu, Y.-D. Fractal Approach to Estimating Changes in Soil Properties Following the Establishment of Caragana Korshinskii Shelterbelts in Ningxia, NW China. *Ecol. Indic.* **2014**, *43*, 236–243. [[CrossRef](#)]
49. Yao, Y.; Liu, J.; Wang, Z.; Wei, X.; Zhu, H.; Fu, W.; Shao, M. Responses of Soil Aggregate Stability, Erodibility and Nutrient Enrichment to Simulated Extreme Heavy Rainfall. *Sci. Total Environ.* **2020**, *709*, 136150. [[CrossRef](#)] [[PubMed](#)]
50. Luo, T.; Liu, W.; Xia, D.; Xia, L.; Guo, T.; Ma, Y.; Xu, W.; Hu, Y. Effects of Land Use Types on Soil Erodibility in a Small Karst Watershed in Western Hubei. *PeerJ* **2022**, *10*, e14423. [[CrossRef](#)]
51. Vaezi, A.R.; Sadeghi, S.H.R.; Bahrami, H.A.; Mahdian, M.H. Modeling the USLE K-Factor for Calcareous Soils in Northwestern Iran. *Geomorphology* **2008**, *97*, 414–423. [[CrossRef](#)]
52. Schmidt, S.; Ballabio, C.; Alewell, C.; Panagos, P.; Meusburger, K. Filling the European Blank Spot—Swiss Soil Erodibility Assessment with Topsoil Samples. *J. Plant Nutr. Soil Sci.* **2018**, *181*, 737–748. [[CrossRef](#)]
53. García-Ruiz, J.M.; Beguería, S.; Nadal-Romero, E.; González-Hidalgo, J.C.; Lana-Renault, N.; Sanjuán, Y. A Meta-Analysis of Soil Erosion Rates across the World. *Geomorphology* **2015**, *239*, 160–173. [[CrossRef](#)]
54. Chen, J.; Li, Z.; Xiao, H.; Ning, K.; Tang, C. Effects of Land Use and Land Cover on Soil Erosion Control in Southern China: Implications from a Systematic Quantitative Review. *J. Environ. Manage.* **2021**, *282*, 111924. [[CrossRef](#)] [[PubMed](#)]
55. Li, Z.-W.; Zhang, G.-H.; Geng, R.; Wang, H.; Zhang, X.C. Land Use Impacts on Soil Detachment Capacity by Overland Flow in the Loess Plateau, China. *Catena* **2015**, *124*, 9–17. [[CrossRef](#)]
56. Zhou, H.; Peng, X.; Peth, S.; Xiao, T.Q. Effects of Vegetation Restoration on Soil Aggregate Microstructure Quantified with Synchrotron-Based Micro-Computed Tomography. *Soil Tillage Res.* **2012**, *124*, 17–23. [[CrossRef](#)]
57. Pérès, G.; Cluzeau, D.; Menasseri, S.; Soussana, J.F.; Bessler, H.; Engels, C.; Habekost, M.; Gleixner, G.; Weigelt, A.; Weisser, W.W.; et al. Mechanisms Linking Plant Community Properties to Soil Aggregate Stability in an Experimental Grassland Plant Diversity Gradient. *Plant Soil* **2013**, *373*, 285–299. [[CrossRef](#)]
58. Erktan, A.; Cécillon, L.; Graf, F.; Roumet, C.; Legout, C.; Rey, F. Increase in Soil Aggregate Stability along a Mediterranean Successional Gradient in Severely Eroded Gully Bed Ecosystems: Combined Effects of Soil, Root Traits and Plant Community Characteristics. *Plant Soil* **2016**, *398*, 121–137. [[CrossRef](#)]
59. Adhikary, P.P.; Tiwari, S.P.; Mandal, D.; Lakaria, B.L.; Madhu, M. Geospatial Comparison of Four Models to Predict Soil Erodibility in a Semi-Arid Region of Central India. *Environ. Earth Sci.* **2014**, *72*, 5049–5062. [[CrossRef](#)]

60. Adesodun, J.; Adeyemi, E.; Oyegoke, C. Distribution of Nutrient Elements within Water-Stable Aggregates of Two Tropical Agro-Ecological Soils under Different Land Uses. *Soil Tillage Res.* **2007**, *92*, 190–197. [[CrossRef](#)]
61. He, Y.; Sheng, M.; Wang, K.; Wang, L. Effects of Land Use Change on Constitution, Stability, and C, N, P Stoichiometric Characteristics of Soil Aggregates in Southwest China. *Environm. Sci.* **2022**, *43*, 3752–3762. (In Chinese) [[CrossRef](#)]

**Disclaimer/Publisher’s Note:** The statements, opinions and data contained in all publications are solely those of the individual author(s) and contributor(s) and not of MDPI and/or the editor(s). MDPI and/or the editor(s) disclaim responsibility for any injury to people or property resulting from any ideas, methods, instructions or products referred to in the content.